Supporting Information for:

Photophysical properties of push-pull 8-aryl-deoxyguanosine probes within duplex and G-quadruplex structures

Darian J. M. Blanchard,[a] *Kaila L. Fadock,*[a] *Michael Sproviero,*[a] *Prashant Deore,*[a] *Richard A. Manderville,*[a,*] *Purshotam Sharma,*[b,c] *and Stacey D. Wetmore*[*,b]

[a]Department of Chemistry, University of Guelph, Guelph, Ontario, Canada, N1G 2W1; [b]Department of Chemistry, University of Lethbridge, Lethbridge, Alberta, Canada, T1K 3M4; and [c]Centre for Computational Sciences, Central University of Punjab, Bathinda, Punjab, 151001, India.

Table of Contents

Table S1. Chemical shifts (δ) of H2′, C1′, C2′, C3′ and C4′ of C8-aryl-dG probes and dG in DMSO-d_6.

Probe	δ H2′	δ C1′	δ C2′	δ C3′	δ C4′
dG	2.50	82.5	39.5	70.7	87.5
BthdG	3.22	84.2	36.7	70.7	87.8
AcphdG	3.14	84.7	36.5	71.2	87.9
QdG	3.18	85.5	38.0	71.2	87.8
PydG	3.47	85.3	37.8	71.2	88.0
vBthdG	2.60	82.8	41.2[b]	71.0	87.7
vAcphdG	2.59[b]	82.9	41.2[b]	70.7	87.8

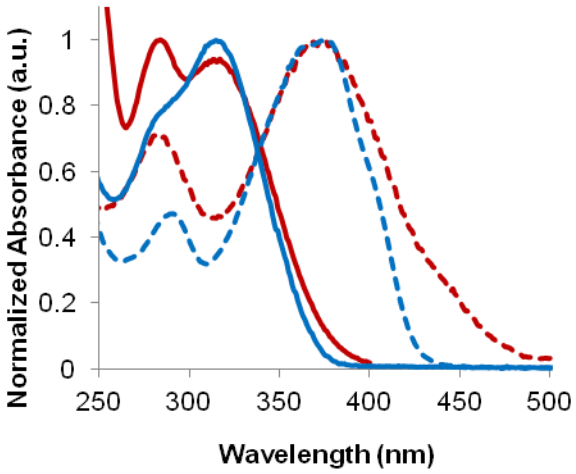

Fig. S1. Absorption spectra of AcphdG (solid red trace), vAcphdG (dashed red trace), BthdG (solid blue trace), and vBthdG (dashed blue trace) in 10 mM aqueous MOPS buffer pH 7, μ = 0.1 M NaCl.

Table S2. Photophysical properties of 8-aryl-dG probes in 80% glycerol:20% aqueous buffer compared to water.

Probe	λ_{em} (nm) H_2O	λ_{em} (nm) 80% glycerol	$\Delta\lambda_{em}$ (nm)	I_{rel}
BthdG	419	413	−6	0.25
AcphdG	419	421, 517	8	6.1/35
QdG	407	421, 456	14	2.7/7.3
PydG	482	476	−6	5.1
vBthdG	473	470	−3	6.6
vAcphdG	488	478	−10	49.5

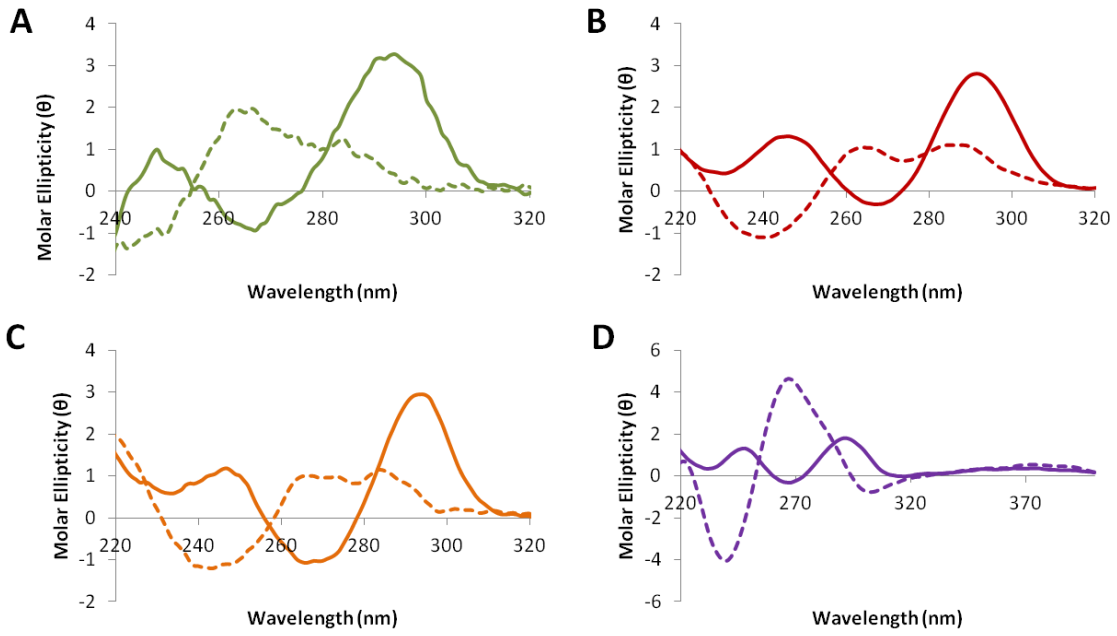

Fig. S2. CD spectra of (A) vAcphdG-mTBA, (B) vBthdG-mTBA, (C) QdG-mTBA, and (D) PydG-mTBA with probe in G_5 in duplex (dashed traces) and GQ (solid traces).

Experimental Section.

Synthesis of Phosphoramidites. Phosphoramidites of BthdG,[1] PydG,[1] QdG[2] and vBthdG[3] were available in our laboratory and were synthesized according to the strategy outlined in Scheme S1. The same procedure was also utilized for conversion of AcphdG and vAcphdG into phosphoramidites for mTBA synthesis using solid-phase synthesis.

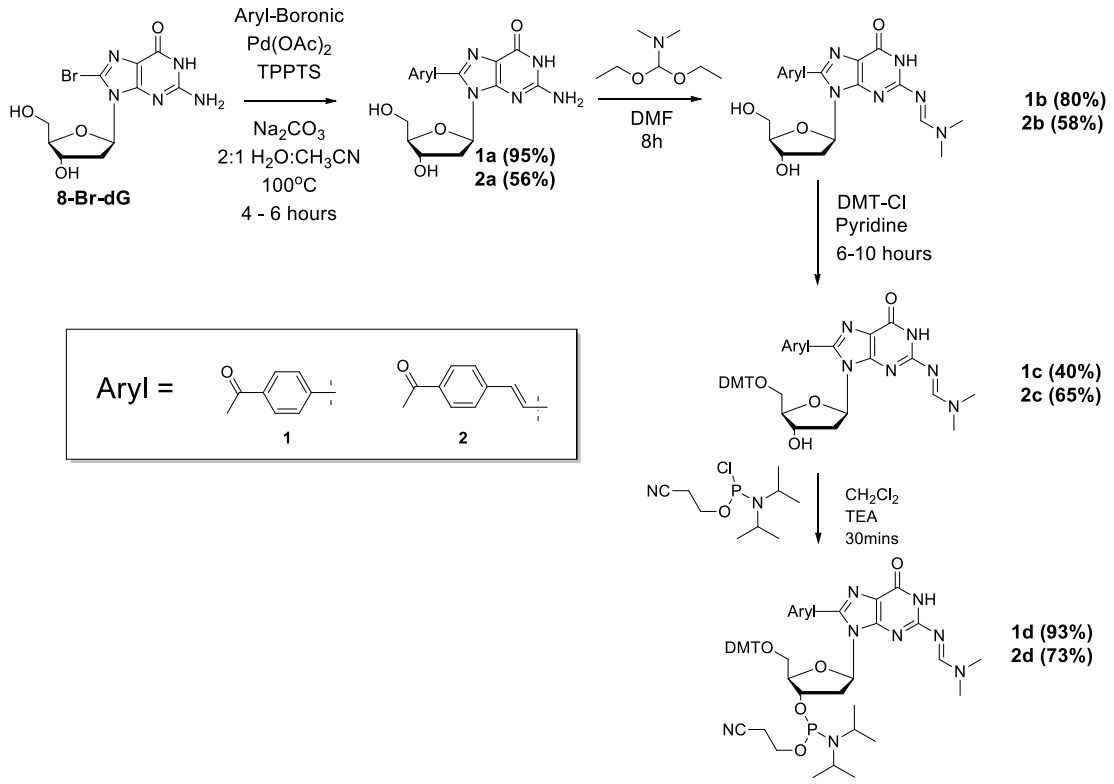

Scheme S1. Phosphoramidite Synthesis

General Procedure for synthesis of 8-Aryl-2'-deoxyguanonosine. $Pd(OAc)_2$ (0.15 mmol), TPPTS (0.3 mmol), Na_2CO_3 (15 mmol), and aryl boronic ester (3.6 mmol) were placed in a round bottomed flask fitted with a condenser and reverse filled with argon. Degassed 2:1 H_2O:CH_3CN (35 mL) solution was added and the solution was heated to reflux for 4-5 hours. Following completion the mixture was diluted with 200 mL of H_2O

and pH was adjusted to 7.5 with 1.0 M aqueous HCl. The mixture was then cooled to 0^{o}C, filtered, washed with DCM and dried to yield product.

8-(4"-acetylphenyl)-2'-dG (1a): Synthesis was performed as described. (Yield 95%). ^{1}H NMR (300 MHz, DMSO-d_6) δ =10.77 (bs, 1H), 8.09 (d, J= 8.4 Hz, 2H), 7.82 (d, J= 8.4 Hz, 2H), 6.45 (bs, 1H), 6.10 (t, J=7.8 Hz, 1H), 5.14 (d, J= 4.5 Hz, 1H), 4.95 (t, J= 6.0 Hz, 1H), 4.34 (m, 1H), 3.78 (m, 1H), 3.62 (m, 1H), 3.55 (m, 1H), 3.14 (m, 1H), 2.62 (s, 3H), 2.02 (m, 1H). ^{13}C NMR (300 MHz, DMSO-d_6) δ = 197.5, 156.6, 153.1, 152.3, 146.0, 136.9, 134.5, 129.3, 128.5, 118.9, 87.9, 84.7, 71.2, 61.9, 36.5, 27.0. HRMS calcd for $C_{18}H_{19}N_5O_5^+$ [M+H$^+$] 386.1464; found 386.1459.

8-(4"-acetylstyrene)-2'-dG (2a): Synthesis was performed as described. (Yield 56%). ^{1}H NMR (400 MHz, DMSO-d_6) δ = 10.78 (bs, 1H), 7.95 (d, J = 8.4 Hz, 1H), 7.82 (d, J = 8.4 Hz, 1H), 7.67 (d, J = 15.9 Hz, 1H), 7.57 (d, J = 15.9 Hz, 1H), 6.59 (bs, 2H), 6.38 (m, 1H), 5.34 (d, J = 4.1, 1H), 5.29 (t, J = 10.4, 1H), 4.47 (m, 1H), 3.85 (m, 1H), 3.71 (m, 2H), [obscured view of H2'], 2.59 (s, 1H), 2.11 (m, 1H); ^{13}C NMR (100 MHz, DMSO-d_6) δ = 197.9, 157.5, 154.3, 152.3, 144.3, 141.3, 136.4, 132.0, 129.2, 127.8, 119.0, 117.3, 87.8, 82.9, 70.7, 61.7, 27.2. HRMS calcd for $C_{20}H_{21}N_5O_5^+$ [M+H$^+$] 412.1622; found 412.1612.

General Procedure for N^2 Protection. A typical procedure involved placing 8-aryl-2′-deoxyguanosine (3.3 mmol) in a round bottomed flask (RBF) and reverse filled with argon. 15 mL of dry DMF was added followed by dimethyl-formamide-diethyl-acetal (2.7 mL, 13.5 mmol) and the mixture was allowed to stir until completion overnight at room temperature. The reaction mixture was then evaporated to dryness and the solid

washed with MeOH and dried to yield product which was converted quantitatively and able to be used without further purification.

***N*^{2}-(dimethylformamidyl)-8-(4"-acetylphenyl)-2'-dG (1b):** Synthesis performed as outlined (80% yield).). ^{1}H NMR (300 MHz, DMSO-d_6) δ= 11.52 (bs, 1H), 8.51 (s, 1H), 8.11 (d, J= 7.5 Hz, 2H), 7.83 (d, J= 7.8 Hz, 2H), 6.14 (t, J= 6.6 Hz, 1H), 5.22 (s, 1H), 4.88 (s, 1H), 4.44 (s, 1H), 3.81 (s, 1H), 3.67 (m, 1H), 3.58 (m, 1H), 3.15 (s, 3H), 3.04 (s, 3H), 2.63 (s, 3H), 2.07 (m, 1H). ^{13}C NMR (300 MHz, DMSO-d_6) δ = 197.5, 158.2, 157.5, 157.0, 150.9, 147.0, 137.0, 134.3, 129.4, 128.4, 120.5, 87.8, 84.9, 71.0, 61.9, 40.8, 37.0, 34.7, 26.9. HRMS calcd for $C_{22}H_{24}N_6O_5^+$ [M+H$^+$] 441.1886; found 441.1896.

***N*^{2}-(dimethylformamidyl)-8-(4″-acetylstyrene)-2′-dG (2b):** Synthesis performed as outlined (58% yield). ^{1}H NMR (400 MHz, DMSO-d_6) δ = 11.46 (bs, 1H), 8.57 (s, 1H), 7.95 (d, J= 8.2, 2H), 7.86 (d, J=8.3 Hz, 2H), 7.70 (d, J=15.9 Hz, 1H), 7.64 (d, J= 15.9 Hz, 1H), 6.52 (t, J=10.1 Hz, 1H), 5.38 (d, J=4.1 Hz, 1H), 5.21 (t, J=10.1, 1H), 4.42 (m, 1H), 3.83 (m, 1H), 3.74 (m, 1H), 3.66 (m, 1H), 3.17 (s, 3H), 3.04 (s, 3H), 2.69 (m, 1H), 2.59 (s, 1H), 2.17, (m, 1H). ^{13}C NMR (100 MHz, DMSO-d_6): 197.8, 158.6, 157.7, 157.5, 150.9, 145.4, 141.2, 136.5, 132.7, 129.2, 127.9, 126.0, 120.4, 118.7, 87.6, 82.9, 70.5, 61.5, 41.2, 35.1, 27.2. HRMS Calcd for $C_{23}H_{26}N_6O_5^+$ [M+H$^+$] 467.2044; found 467.2038.

General Procedure for 5′-OH Protection. *N*^{2}-(Dimethylformamidyl)-8-aryl-2′-dG (2.7 mmol) was co-evaporated from dry pyridine (3 x 5 mL) in a RBF. The RBF was then fitted with a constant pressure dropping funnel, reverse filled with argon, and 7 mL of dry pyridine (or DMF) was added to the RBF and cooled to 0^{o}C. A DMT-Cl (1.28 g, 3.78 mmol) pyridine (5 mL) solution was added to the dropping funnel under argon and allowed to add dropwise over 30 min. The reaction was allowed to stir at room

temperature under argon and was monitored by TLC. Upon completion, the mixture was diluted with methylene chloride (10 mL) and washed with water (2 x 10 mL). TEA (1 mL) was added and the mixture was evaporated to yield an oil. The oil was then loaded onto a silica column and run with 95:5 CH_2Cl_2:TEA to elute unreacted DMT material; product was then eluted with MeOH:CH_2Cl_2:TEA (5:90:5), fractions deemed pure were combined and rotovapped to yield a powder.

5′-O-(4,4′-dimethoxytrityl)-N^2-(dimethylformamidyl)-8-(4′′-acetylphenyl)-2′-dG (1c): Synthesis performed as outlined. (40% yield). ^{1}H NMR (300 MHz, $CDCl_3$) δ = 8.36 (s, 1H), 7.98-7.95(d, 2H, J= 8.7 Hz), 7.94-7.91 (d, 2H, J= 8.7 Hz), 7.40-7.37 (m, 2H), 7.28-7.24 (m, 4H), 7.20-7.13 (m, 3H), 6.73-6.70 (m, 4H), 6.21-6.14 (m, 1H), 4.83-4.79 (m, 1H), 4.10-4.05 (m, 1H), 3.73 (s, 6H), 3.51-3.44 (m, 1H), 3.38-3.24 (m, 2H), 2.99 (s, 3H), 2.90 (s, 3H), 2.60 (s, 3H), 2.31-2.24 (m, 1H). ^{13}C NMR (400 MHz, $CDCl_3$) δ= 197.6, 158.3, 158.2, 158.0, 157.9, 155.8, 151.3, 148.5, 144.8, 137.3, 135.9, 135.8, 129.9, 129.8, 129.7, 128.3, 128.0, 127.7, 126.7, 120.7, 112.9, 86.0, 85.3, 84.0, 72.0, 64.2, 55.2, 52.7, 45.9, 41.4, 37.9, 35.1, 26.8, 9.8, 7.9. HRMS calcd for [M + H^+]: 743.3139 found 743.3211.

5′-O-(4,4′-dimethoxytrityl)-N^2-(dimethylformamidyl)-8-(4′′-acetylstyrene)-2′-dG (2c): Synthesis performed as outlined. (65% yield). ^{1}H NMR (400 MHz, $CDCl_3$) δ = 9.26 (bs, 1H), 8.45 (s, 1H), 7.86 (d, J=15.9, 1H), 7.77 (d, J= 8.0 Hz, 2H), 7.39 (m, 4H), 7.70 (s, 1H), 7.28 (m, 5H), 7.18 (m, 4H), 6.73 (m, 4H), 6.52 (t, J = 12.5, 1H), 4.77 (bs, 1H), 4.17 (d, J= 4.6 Hz, 1H), 3.71 (s, 3H), 3.70 (s, 3H), 3.50 (m, 1H), 3.41 (m, 1H), 3.14 (m, 1H), 3.05 (s, 3H), 3.04 (s, 3H), 2.48 (m, 1H). ^{13}C NMR (100 MHz, $CDCl_3$) δ= 197.6, 158.4, 158.0, 157.7, 156.0, 150.8, 146.4, 144.6, 140.6, 136.4, 135.7, 135.6, 134.1, 130.0,

129.9, 128.8, 128.1, 127.8, 127.1, 126.9, 120.5, 116.8, 113.1, 86.3, 85.2, 83.0, 72.4, 64.3, 55.1, 46.0, 41.4, 39.2, 35.2, 26.7. HRMS calcd for [M + H^+] 769.3350, found 769.3337.

Phosphoramidite Reaction. The 5′-*O*-DMT(DMPx)-N^2-(dimethylformamidyl)-8-aryl-2′-dG (0.706 mmol) was co-evaporated from dry THF (3 x 5 mL), reverse filled with argon and dissolved in 10 mL dry, degassed CH_2Cl_2. To this was added dry, degassed TEA (0.4 mL, 2.83 mmol) and 2-cyanoethyl *N*,*N*-diisopropylchlorophosphoramidite (0.24 mL, 1.06 mmol). The reaction was monitored via TLC and, upon completion (20-40 min), was washed successively with saturated, degassed sodium bicarbonate solution. The organic phase was separated, dried with Na_2SO_4 and purified by a combination of re-crystallization, by initially dissolving in methylene chloride and dripping into hexanes at -78°C, and flash chromatography, by loading onto a flash chromatography column eluting with 92:5:3 CH_2Cl_2:MeOH:TEA. Phosphoramidites were isolated as their corresponding diastereomers, and were characterized by ^{31}P NMR and HRMS. The two amidites were ~ 60% pure based on ^{31}P NMR analysis with a P(V) derivative (δ 14.3 ppm) as the major impurity.

3′-O-[(2-Cyanoethoxy)(diisopropylamino)phosphino]-5′-*O*-(4,4′-dimethoxytrityl)-N^2-(dimethylformamidyl)-8-(4′′-acetylphenyl)-2′-dG (1d): Synthesis performed as outlined. (93% yield). ^{31}P NMR (121 MHz, $CDCl_3$) δ = 149.0, 148.9. HRMS calcd for $C_{51}H_{60}N_8O_8P^+$ [M+H^+]: 943.4272; found 943.4236.

3′-O-[(2-Cyanoethoxy)(diisopropylamino)phosphino]-5′-*O*-(4,4′-dimethoxytrityl)-N^2-(dimethylformamidyl)-8-(4′′-acetylstyrene)-2′-dG (2d): Synthesis performed as outlined. (73% yield). ^{31}P NMR (121 MHz, $CDCl_3$) δ = 149.1, 148.9. HRMS calcd for $C_{53}H_{61}N_8O_8P^+$ [M+H^+]: 969.4429; found 969.4419.

DFT calculations. The preferred conformations of 4-OH-Ph-dG were previously determined by initially performing conformational searches using the Monte Carlo method and the MMFF force field.[4] The ten lowest energy structures identified from the conformational search were subsequently fully optimized with B3LYP/6-31G(d). The resulting lowest energy conformer adopted a C2′-endo puckering, the C5′-hydroxyl group is directed toward the nucleobase, and the C3′-hydroxyl group is directed toward C2′ (∠(HC3′O3′H) approximately equal to –60°). Using this structure as the starting point, a B3LYP/6-31G(d) PES was constructed by constraining the dihedral angles χ and θ in 10° increments from 0° to 360°. Full optimizations of stationary points on the PES were subsequently performed to determine the geometries of the 4-OH-Ph-dG minima and transition states. In the present work, all minima and transition states previously identified for the 4-OH-Ph-dG adduct were used to generate the initial structures for searching the potential energy surfaces of the AcphdG and PydG adducts. The lowest energy (*syn*) minima identified for these adducts at the B3LYP/6-31G(d) level of theory were used to calculate the orbital energies, whereas the lowest energy *anti* and *syn* minima were used to identify the relative energies at the B3LYP/6-311+G(2df,p) level, which include scaled zero-point vibrational energy (ZPVE) corrections. On the other hand, the *anti*/*syn* relative energies, as well as other structural and electronic properties, for the QdG adduct were taken from our previous study carried out at the same level of theory.[5]

For the vAcphdG and vBthdG nucleosides, a conformational search was performed using Hyperchem 8.0.8[6] with the AMBER[7] molecular mechanics force field to determine the preferred conformations about rotatable torsional angles. Specifically, the

conformational search was performed with respect to: χ ($\angle$(O4′C1′N9C4)), θ ($\angle$(N9C8C10C11)), ϕ ($\angle$(C8C10C11C12)), β ($\angle$(C4′C5′O5′H)), ε ($\angle$(C4′C3′O3′H)), υ_0 ($\angle$(C2′C1′O4′C4′)), υ_1 ($\angle$(O4′C1′C2′C3′)), υ_2 ($\angle$(C4′C3′C2′C1′)), υ_3 ($\angle$(O4′C4′C3′C2′)), υ_4 ($\angle$(C1′O4′C4′C3′)), $\psi^{\text{Acphv-dG}}$ ($\angle$(C10C11C12C13)), $\psi^{\text{Bthv-dG}}$ ($\angle$(C10C11C12S)) and $\tau^{\text{Acphv-dG}}$ ($\angle$(C14C15C16C17)). The usage-directed search method[3] was used to generate starting structures. Partial atomic charges for the AMBER force field were obtained using the HF/6-31G(d) method. The 10 lowest energy conformers obtained for each of the two nucleosides were fully optimized with B3LYP/6-31G(d). The resulting gas-phase global minimum, which adopted the *syn* glycosidic orientation for each probe, was used to calculate the orbital energies. The corresponding *anti* conformation was optimized by rotating about the χ torsional angle in the global minimum from *syn* to *anti*, and the structure was reoptimized. The relative energies of the *syn* and *anti* conformations thus obtained were calculated at B3LYP/6-311+G(2df,p), which include scaled ZPVE correction. All electronic structure calculations were performed using Gaussian 09.[8]

References

1. M. Sproviero, A. M. R. Verwey, A. A. Witham, R. A. Manderville, P. Sharma and S. D. Wetmore, *Chem. Res. Toxicol*., 2015, **28**, 1647-1658.

2. M. Sproviero, K. M. Rankin, A. A.Witham and R. A. Manderville, *J. Org. Chem*., 2014, **79**, 692-699.

3. D. J. M. Blanchard, T. Z. Cservenyi and R. A. Manderville, *Chem. Commun*., 2015, DOI:10.1039/C5CC07154B.

4. A. Millen, C. K. McLaughlin, K. M. Sun, R. A. Manderville and S. D. Wetmore, *J. Phys. Chem. B,* 2008, **112**, 3742-3753.

5. M. Sproviero, K. L. Fadock, A. A. Witham, R. A. Manderville, P. Sharma and S. D. Wetmore, *Chem. Sci.,* 2014, **5**, 788-796.

6. HyperChem (TM) Professional 8.0.8, Hypercube, Inc., 1115 NW 4th Street, Gainesville, Florida 32601, USA.

7. W. D. Cornell, P. Cieplak, C. I. Bayly, I. R. Gould, K. M. Merz, Jr., D. M. Ferguson, D. C. Spellmeyer, T. Fox, J. W. Caldwell and P. A. Kollman, *J. Am. Chem. Soc.,* 1995, **117**, 5179–5197.

8. Gaussian 09, Revision A.1, Frisch, M. J.; Trucks, G. W.; Schlegel, H. B.; Scuseria, G. E.; Robb, M. A.; Cheeseman, J. R.; Scalmani, G.; Barone, V.; Mennucci, B.; Petersson, G. A.; Nakatsuji, H.; Caricato, M.; Li, X.; Hratchian, H. P.; Izmaylov, A. F.; Bloino, J.; Zheng, G.; Sonnenberg, J. L.; Hada, M.; Ehara, M.; Toyota, K.; Fukuda, R.; Hasegawa, J.; Ishida, M.; Nakajima, T.; Honda, Y.; Kitao, O.; Nakai, H.; Vreven, T.; Montgomery, Jr., J. A.; Peralta, J. E.; Ogliaro, F.; Bearpark, M.; Heyd, J. J.; Brothers, E.; Kudin, K. N.; Staroverov, V. N.; Kobayashi, R.; Normand, J.; Raghavachari, K.; Rendell, A.; Burant, J. C.; Iyengar, S. S.; Tomasi, J.; Cossi, M.; Rega, N.; Millam, N. J.; Klene, M.; Knox, J. E.; Cross, J. B.; Bakken, V.; Adamo, C.; Jaramillo, J.; Gomperts, R.; Stratmann, R. E.; Yazyev, O.; Austin, A. J.; Cammi, R.; Pomelli, C.; Ochterski, J. W.; Martin, R. L.; Morokuma, K.; Zakrzewski, V. G.; Voth, G. A.; Salvador, P.; Dannenberg, J. J.; Dapprich, S.; Daniels, A. D.; Farkas, Ö.; Foresman, J. B.; Ortiz, J. V.; Cioslowski, J.; Fox, D. J. Gaussian, Inc., Wallingford CT, 2009.

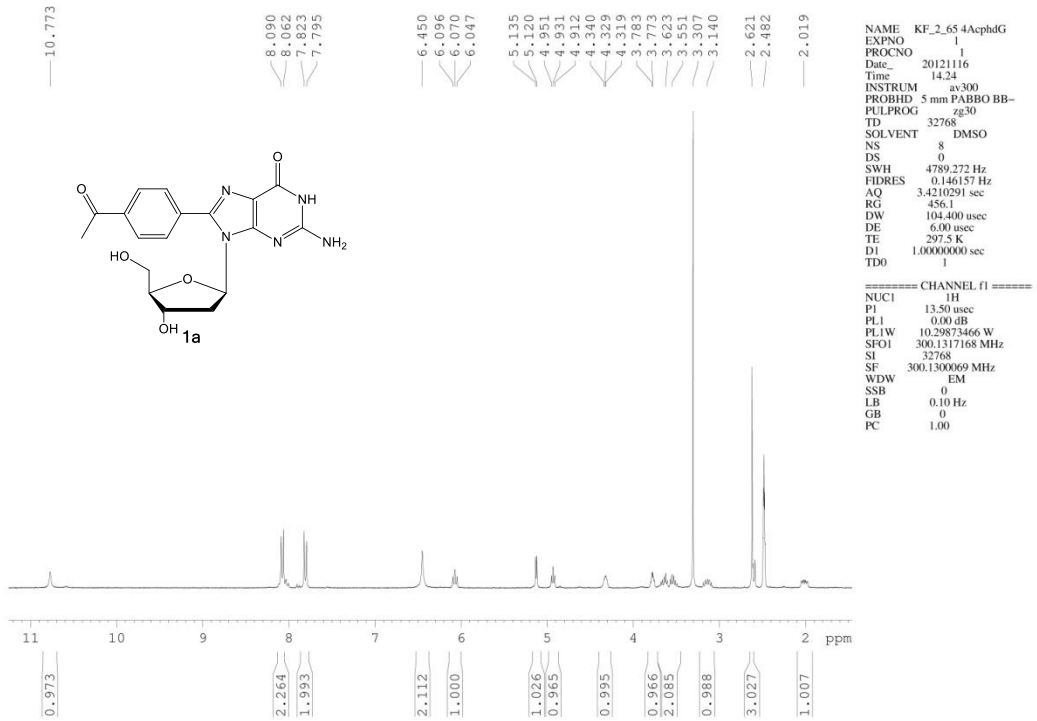

Fig. S3 ^{1}H NMR spectrum of **1a** in DMSO-d_6

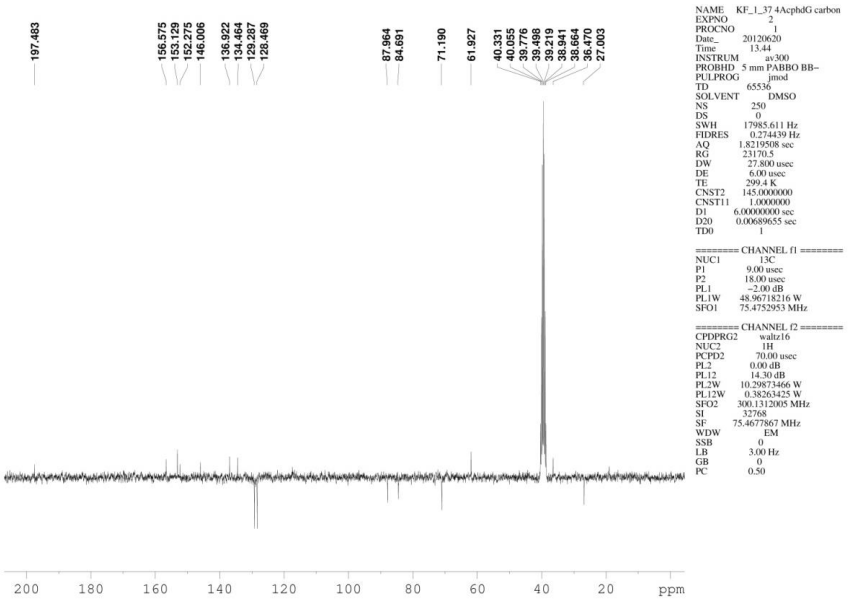

Fig. S4 ^{13}C NMR spectrum of **1a** in DMSO-d_6

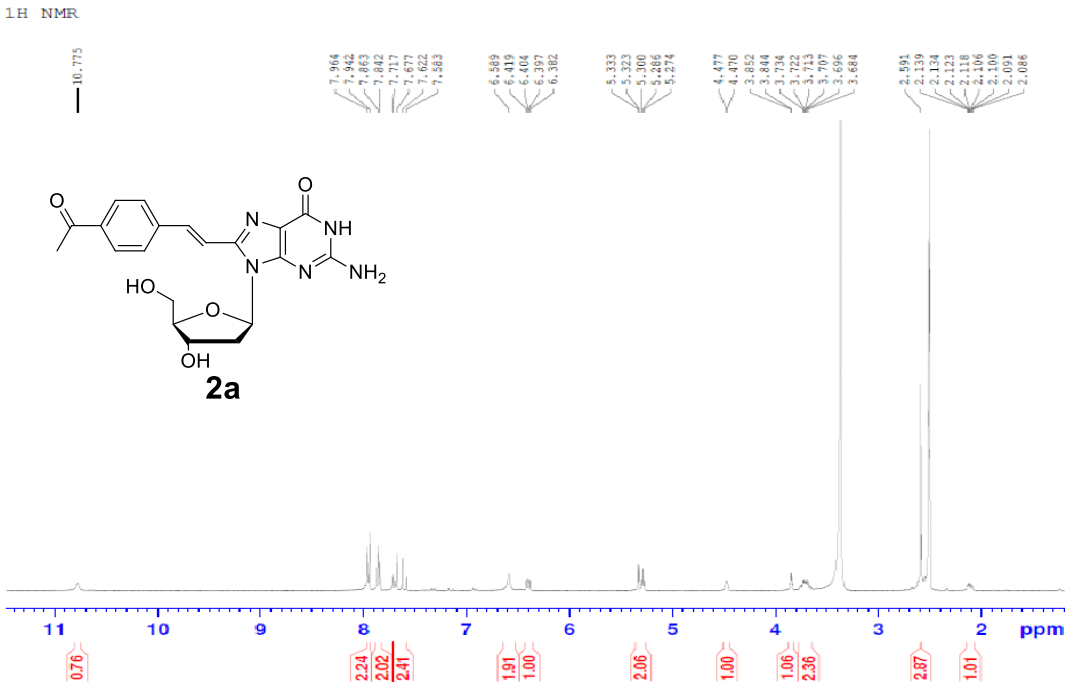

Fig. S5 ^{1}H NMR spectrum of **2a** in DMSO-d_6

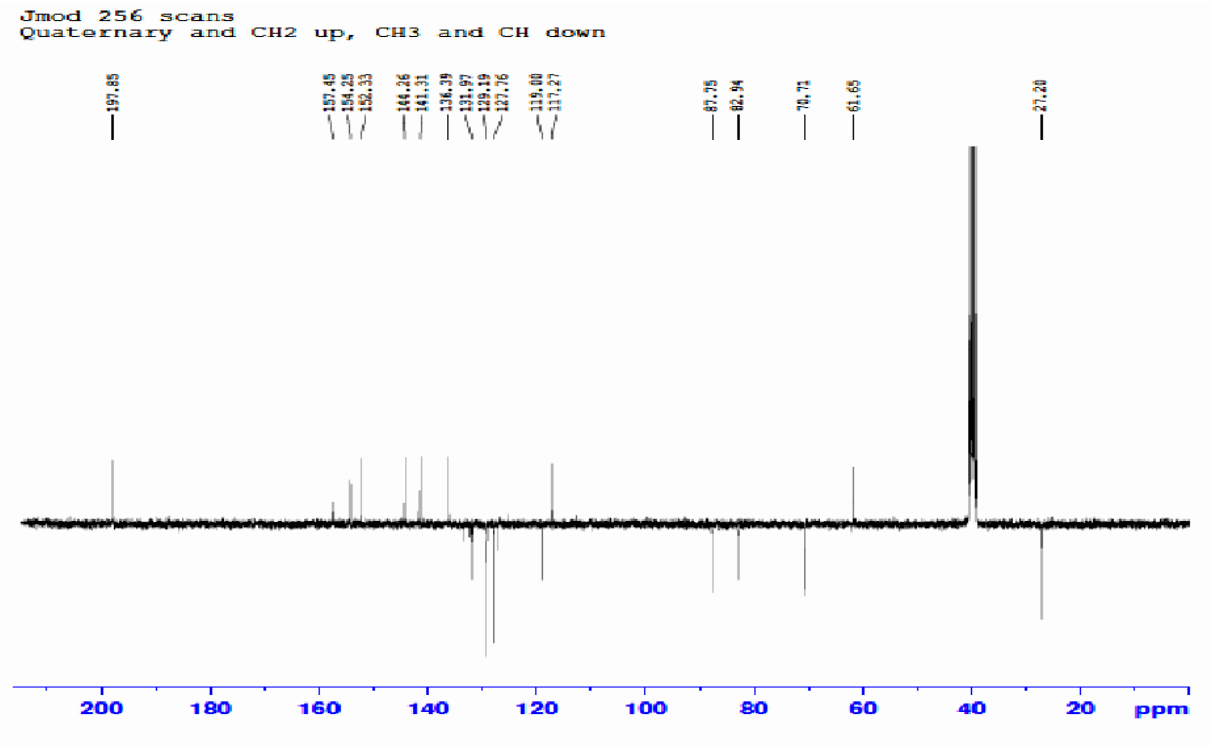

Fig. S6 ^{13}C NMR spectrum of **2a** in DMSO-d_6

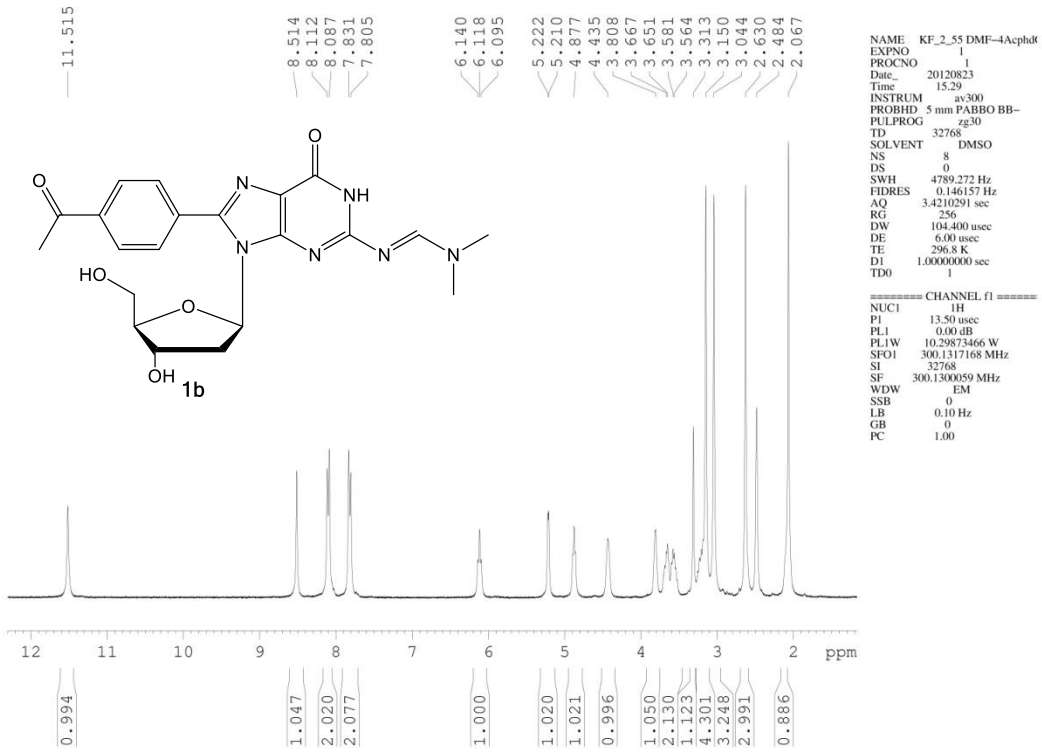

Fig. S7 ^{1}H NMR spectrum of **1b** in DMSO-d_6

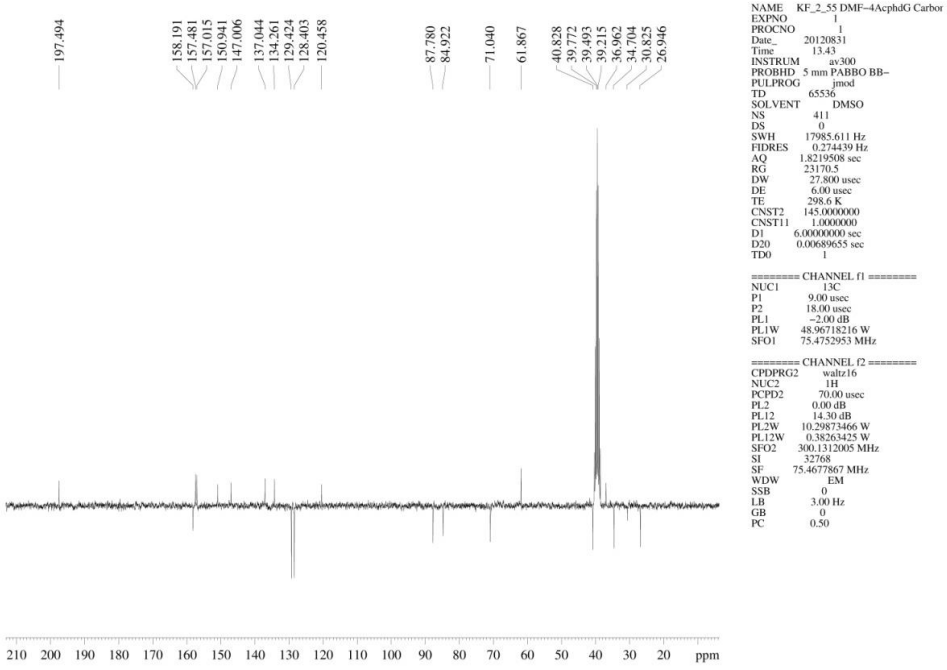

Fig. S8 ^{13}C NMR spectrum of **1b** in DMSO-d_6

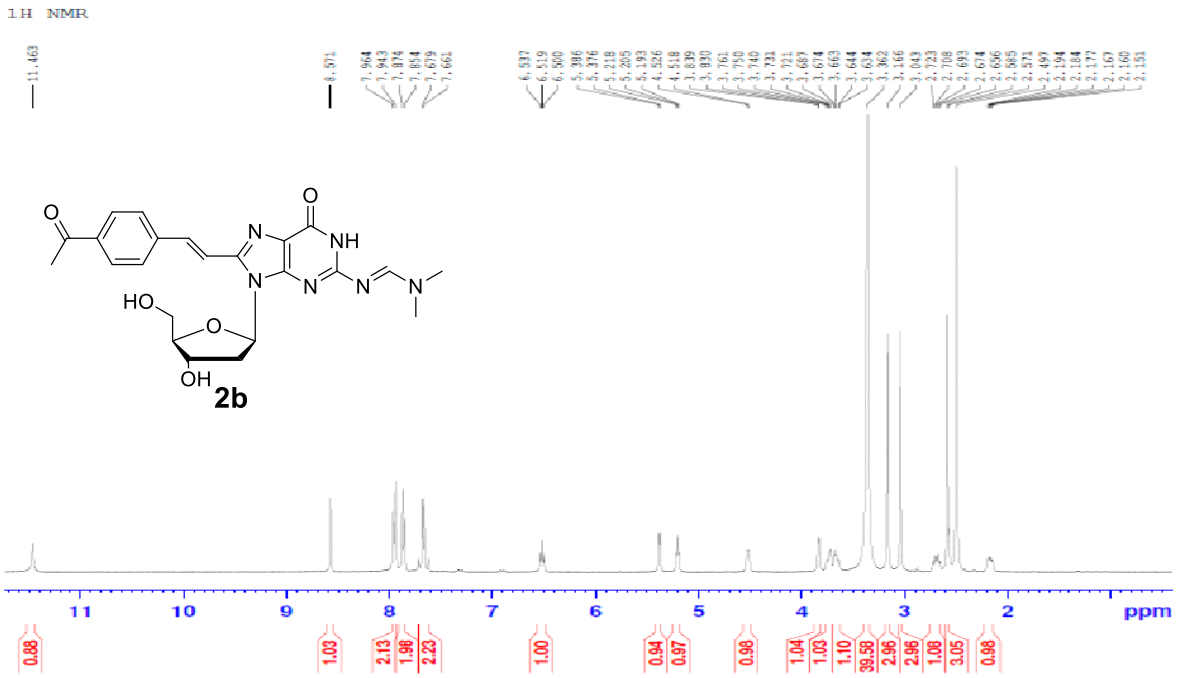

Fig. S9 ^{1}H NMR spectrum of **2b** in DMSO-d_6

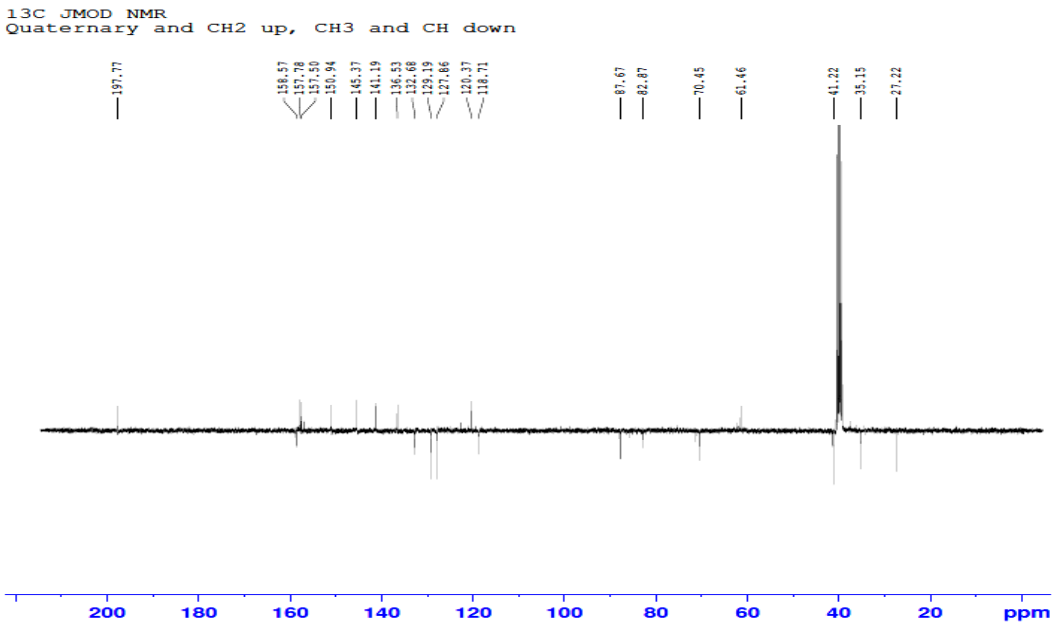

Fig. S10 ^{13}C NMR spectrum of **2b** in DMSO-d_6

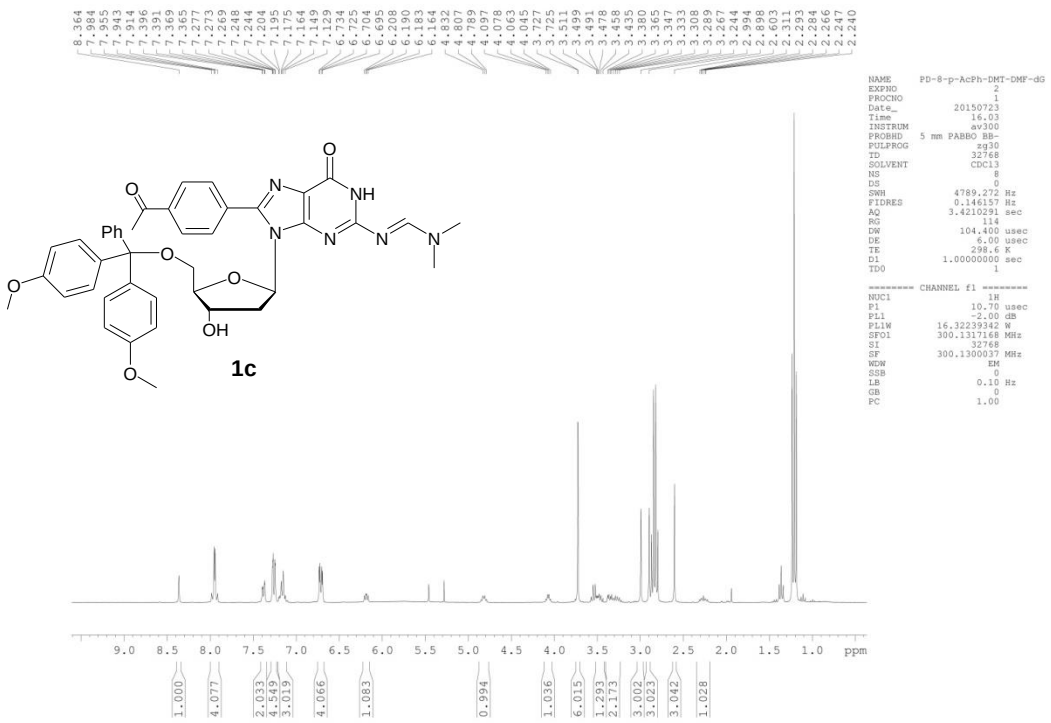

Fig. S11 ^{1}H NMR spectrum of **1c** in $CDCl_3$.

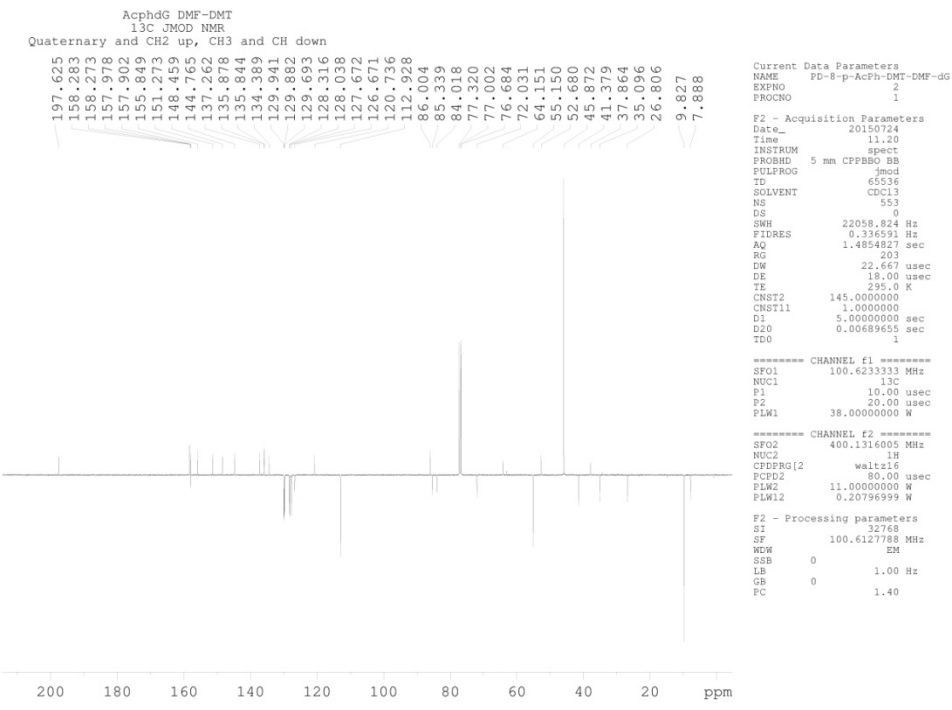

Fig. S12 ^{13}C NMR spectrum of **1c** in $CDCl_3$.

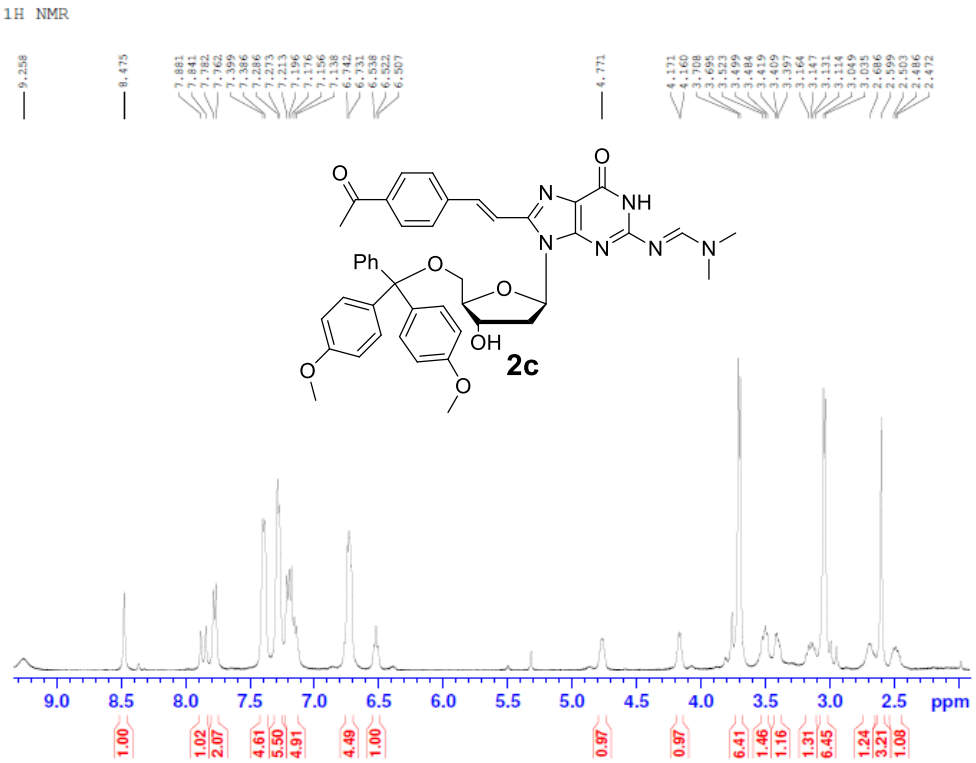

Fig. S13 ^{1}H NMR spectrum of **2c** in $CDCl_3$

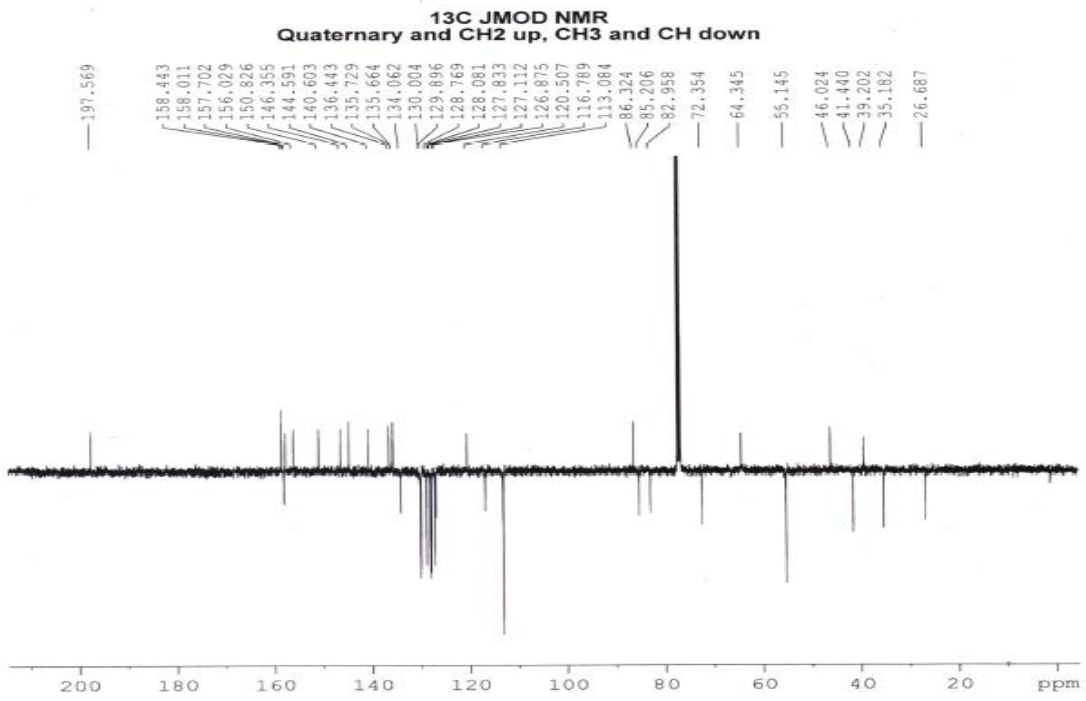

Fig. S14 ^{13}C NMR spectrum of **2c** in $CDCl_3$

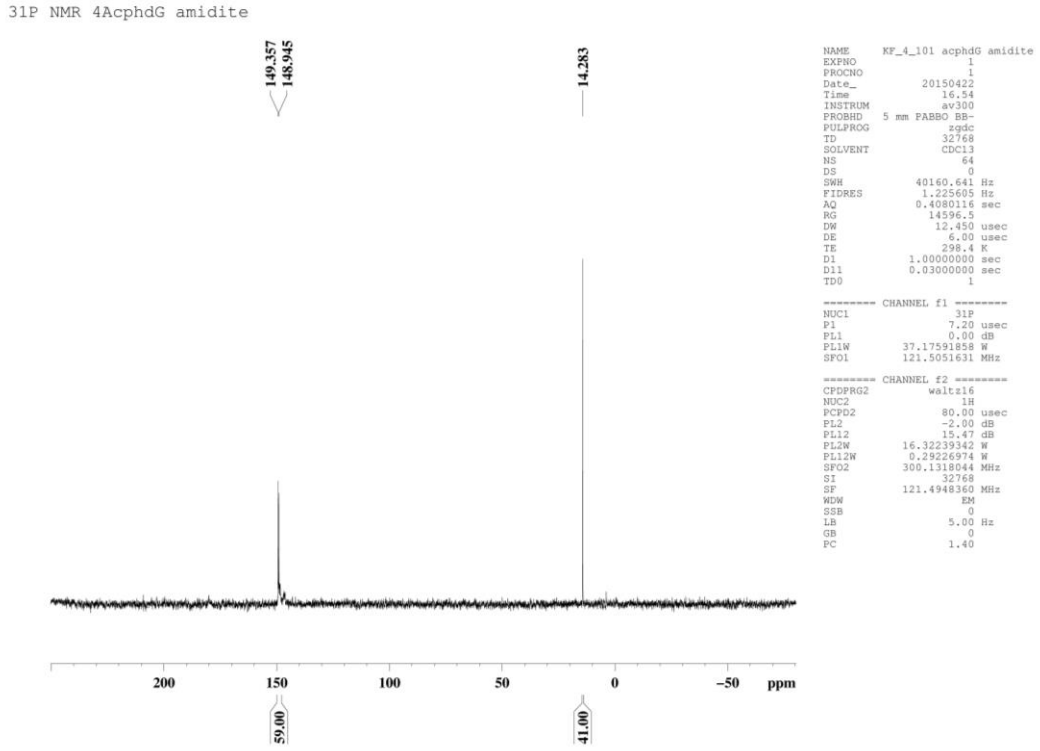

Fig. S15 ^{31}P NMR spectrum of AcphdG amidite in $CDCl_3$

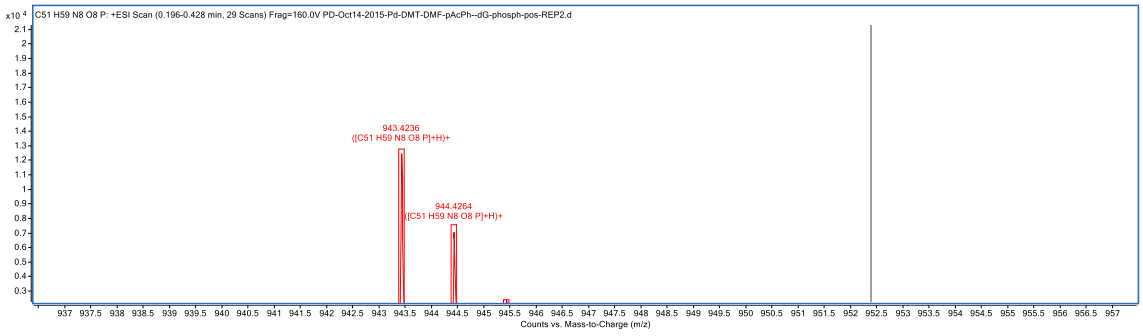

Fig. S16 HRMS of AcphdG amidite

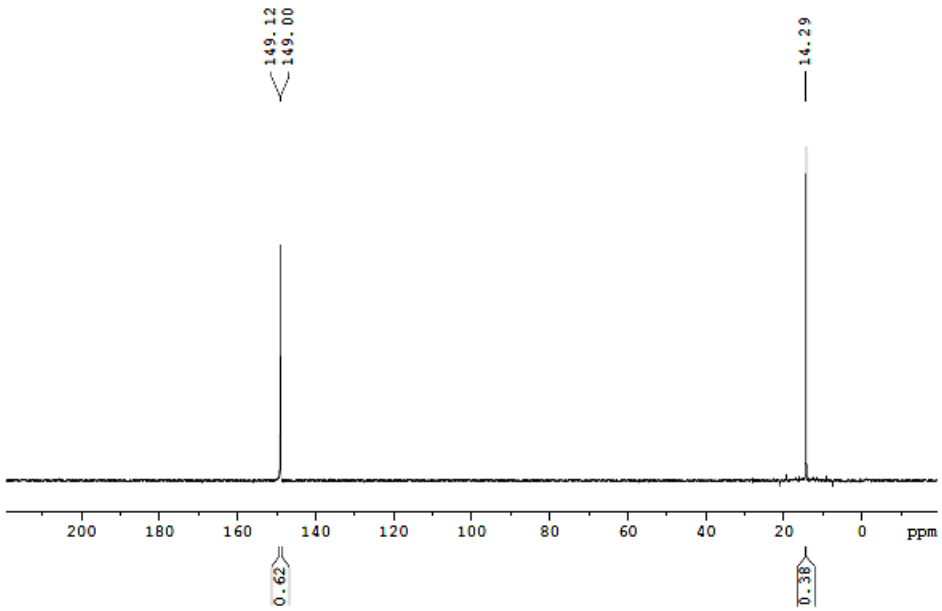

Fig. S17 ^{31}P NMR spectrum of vAcphdG amidite in $CDCl_3$

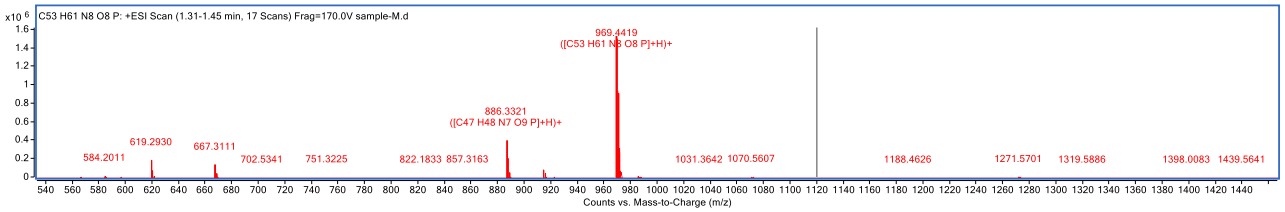

Fig. S18 HRMS of vAcphdG amidite

Table S3: Yields and ESI-MS analysis for mTBA.

probe	Location	Yield (%)[a]	M.W. calcd[b]	M.W. found[c]
AcphdG	5	72	4841.8	4841.0
	6	80	4841.8	4842.9
	8	65	4841.8	4842.8
vAcphdG	5	72	4870.2	4869.9
	6	80	4870.1	4870.4
	8	65	4870.2	4871.0
BthdG	5	69	4855.8	4855.8
	6	66	4855.8	4855.4
	8	74	4855.8	4855.5
vBthdG	5	48	4881.8	4882.5
	6	52	4881.8	4882.3
	8	62	4881.8	4883.0
QdG	5	24	4850.8	4851.0
	6	46	4850.8	4850.9
	8	40	4850.8	4851.1
PydG	5	81	4923.9	4923.6
	8	82	4923.9	4923.8

[a] Yield derived from integration of the semi-preparative HPLC trace following deprotection of the mTBA with concentrated ammonium hydroxide at 55 ° C for 15 h. [b] M.W. of neutral species. [c] ESI-MS analysis and mass deconvoluted for neutral species.

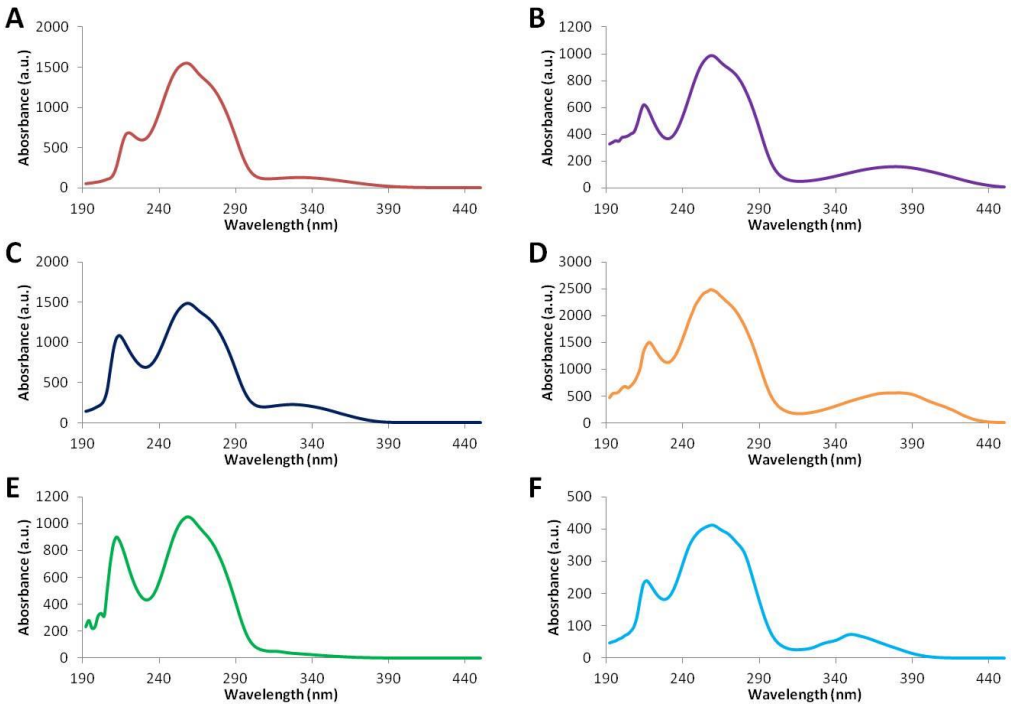

Fig S19 UV traces of (A) AcphdG-, (B) vAcphdG-, (C) BthdG-, (D) vBthdG-, (E) QdG-, and (F) PydG-mTBA.

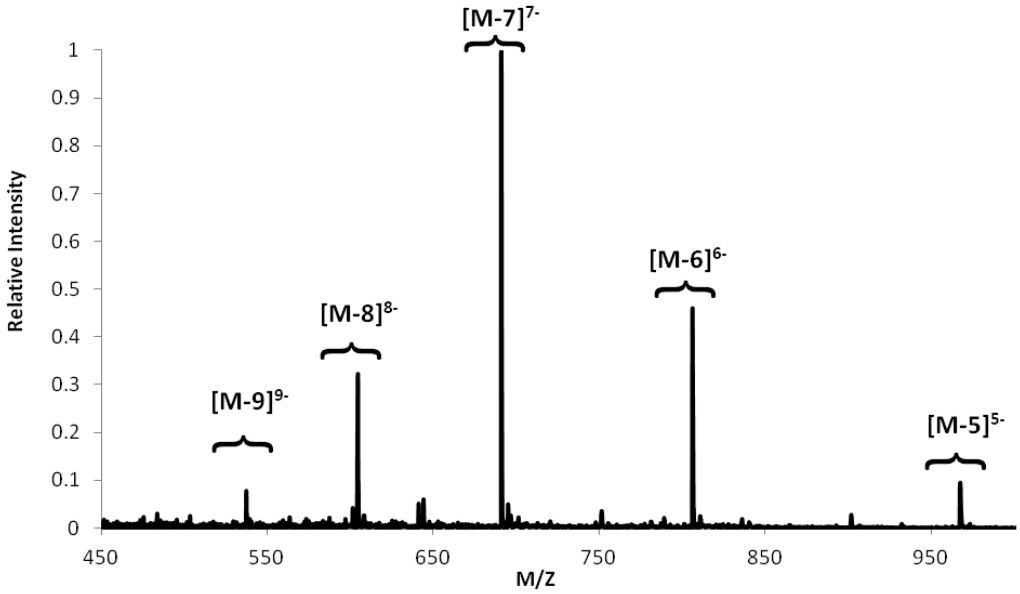

Fig. S20 Mass spectrum of AcphdG-mTBA obtained with an ESI source operated in negative mode.

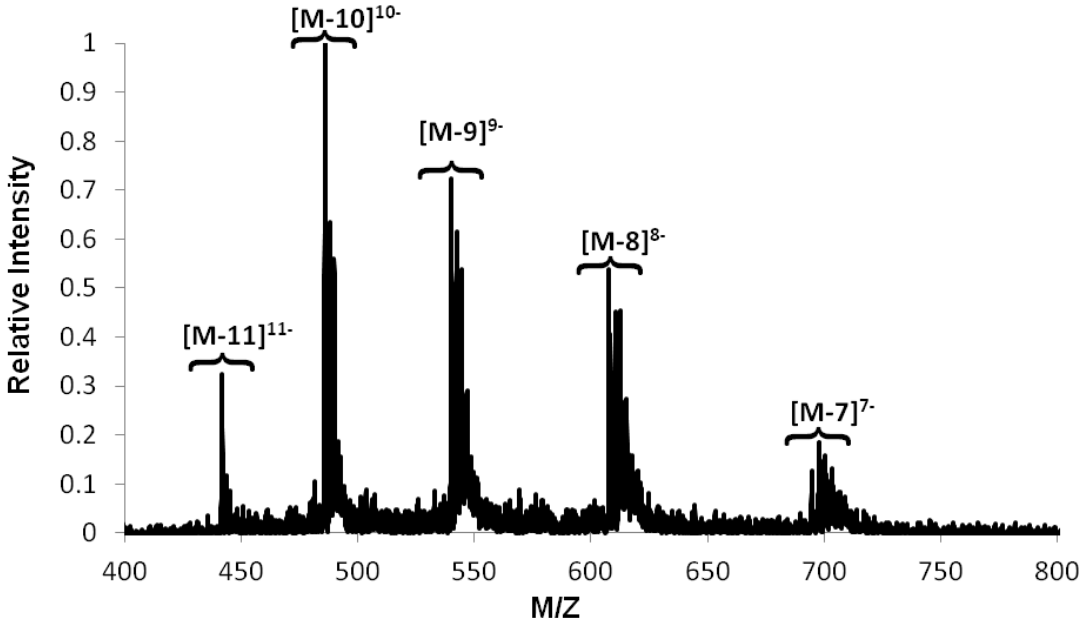

Fig. S21 Mass spectrum of vAcphdG-mTBA obtained with an ESI source operated in negative mode.

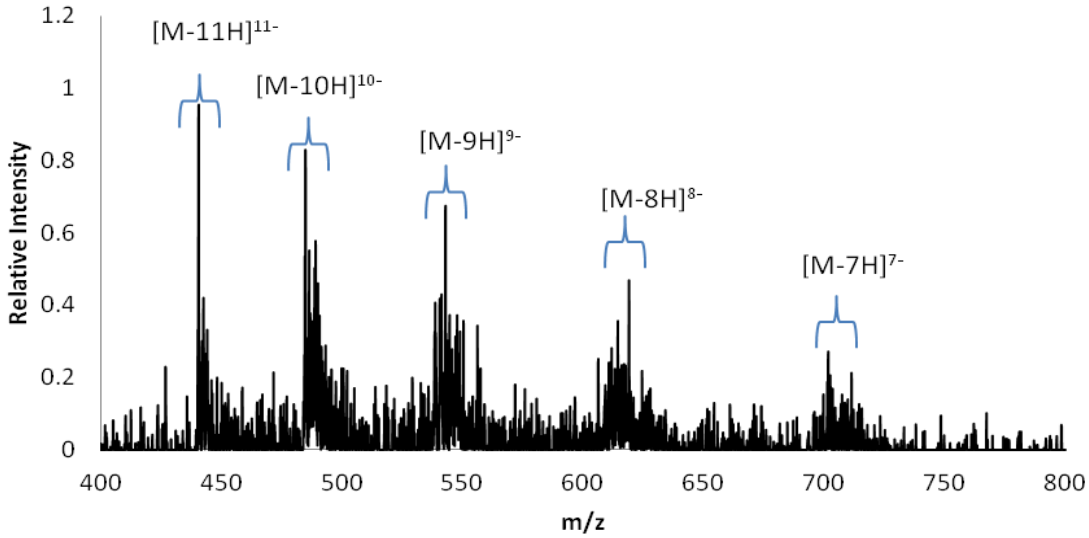

Fig. S22 Mass spectrum of BthdG-mTBA obtained with an ESI source operated in negative mode.

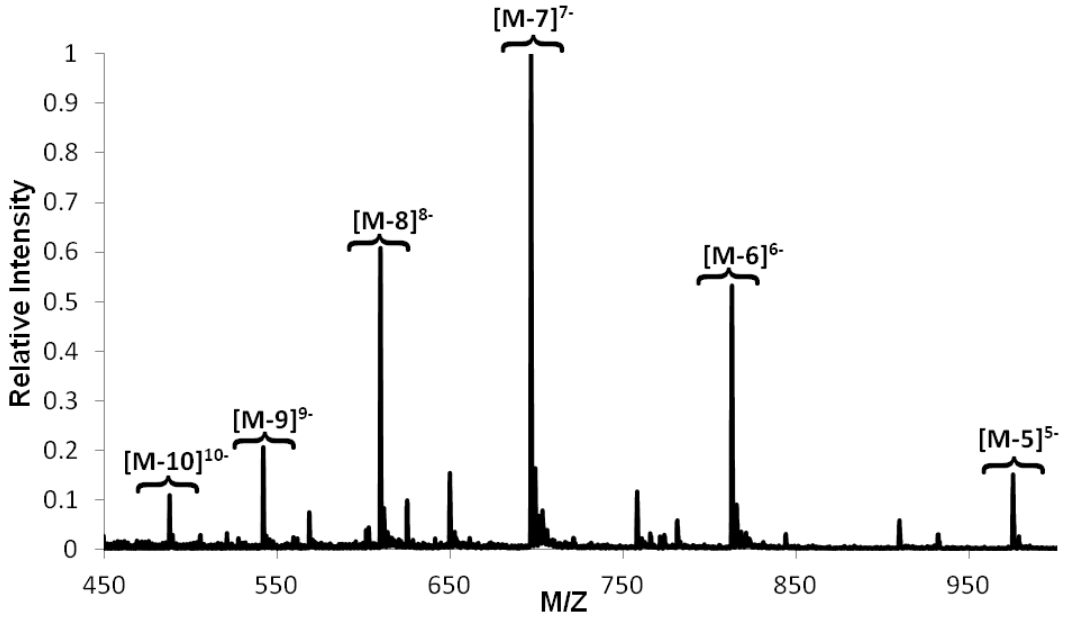

Fig. S23 Mass spectrum of vBthdG-mTBA obtained with an ESI source operated in negative mode.

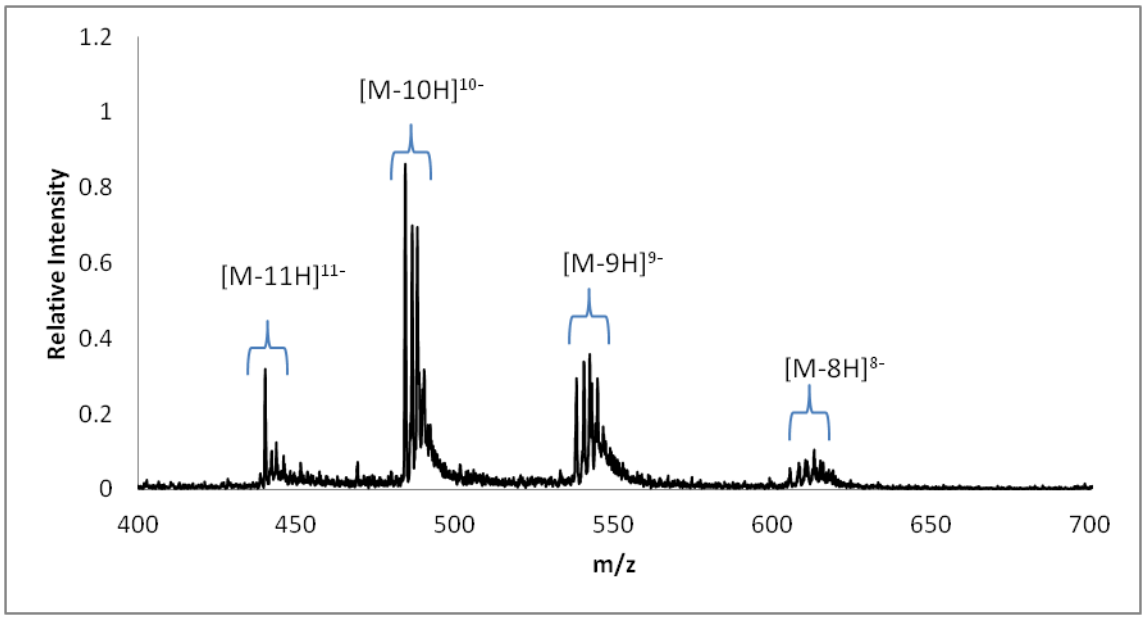

Fig. S24 Mass spectrum of QdG-mTBA obtained with an ESI source operated in negative mode.

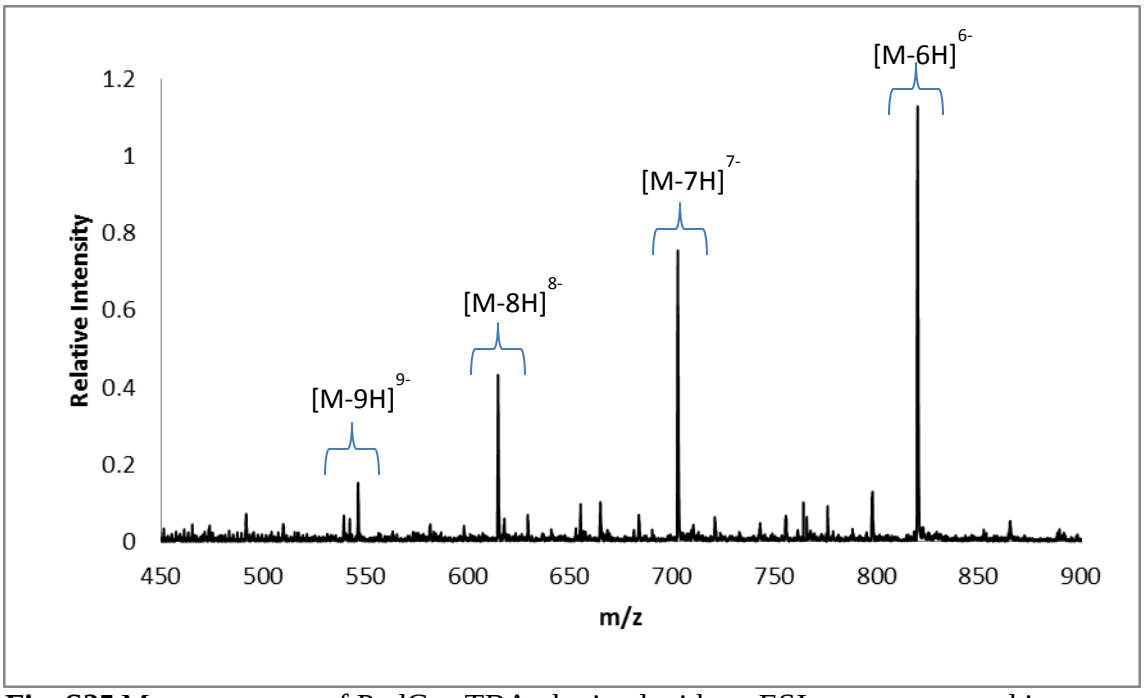

Fig. S25 Mass spectrum of PydG-mTBA obtained with an ESI source operated in negative mode.